



# Fire Behaviour of Rectangular Steel Tubed-Reinforced-Concrete Columns with End Restraints

Dongdong Yang<sup>1,2</sup> · Faqi Liu<sup>3,4</sup> · Shan-Shan Huang<sup>5</sup> · Hua Yang<sup>3,4</sup> · Kun Wang<sup>2</sup>

Received: 21 December 2023 / Accepted: 3 September 2024  
© Korean Society of Steel Construction 2024

## Abstract

The steel tubed-reinforced-concrete (STRC) column is a new form of composite column, in which the steel tube primarily serves to provide confinement to concrete core rather than directly carrying axial force. The restraining effects at the heated column ends should be incorporated into the fire performance design of STRC columns, while current research on rectangular STRC columns is still inadequate. This study presents the numerical study on the fire behaviour of end-restrained rectangular STRC columns. The effects of axial restraint and rotational restraint on the overall deformations, internal forces, fire resistance, axial force and buckling length at fire limit state, of rectangular STRC columns with various cross-sectional sizes, aspect ratios, slenderness ratios and load ratios were thoroughly analyzed. The end-restrained rectangular STRC columns fail in fire mainly due to runaway of axial contraction, and the failure mode may shift from dynamic to static as the axial restraint increases. The fire resistance of rectangular STRC columns subjected to bending around the major axis is generally higher than in the case of minor-axis bending. The axial force inside the column decreases nearly linearly while the fire resistance experiences an almost linear increase with increasing the axial restraint ratio. The beneficial effect of rotational restraint, i.e. decreasing the buckling length and enhancing the fire resistance is prominent, especially for columns under relatively low restraining levels. Finally, simplified equations were given for designing the structural fire performance of rectangular STRC columns with considering the end restraining effects.

**Keywords** Rectangular steel tubed-reinforced-concrete columns · Fire performance · End restraints · Finite element analysis · Buckling length

## 1 Introduction

The steel tubed-reinforced-concrete (STRC) is a new steel-concrete composite column form that comprises an outer steel tube and an inner reinforced concrete (RC) section (Zhou et al., 2023). The steel tube in a STRC column is discontinuous at the joint zone (as shown in Fig. 1), thus it is designed not to carry load axially but to provide sufficient lateral confinement to the concrete. Consequently, the axial load applied onto a STRC mainly acts on the confined RC part. This is significantly different from traditional concrete-filled steel tubular (CFST) columns that may or may not contain internal steel reinforcements; in such cases, the steel tube sustains the axial load together with the inner plain concrete or RC section. The steel tube in a STRC column could confine the concrete core more effectively, and its local buckling is effectively minimized. Owing to the excellent load-bearing capacity, good seismic performance, and construction convenience, STRC columns are increasingly

---

✉ Dongdong Yang  
ddyang@yzu.edu.cn

<sup>1</sup> Zhejiang Engineering Research Center of Intelligent Urban Infrastructure, Hangzhou City University, Hangzhou 310015, China

<sup>2</sup> Department of Civil Engineering, College of Architectural Science and Engineering, Yangzhou University, Yangzhou 225127, China

<sup>3</sup> Key Lab of Structures Dynamic Behaviour and Control, Ministry of Education, Harbin Institute of Technology, Harbin 150090, Heilongjiang, China

<sup>4</sup> Key Lab of Smart Prevention and Mitigation of Civil Engineering Disasters, Ministry of Industry and Information Technology, Harbin Institute of Technology, Harbin 150090, Heilongjiang, China

<sup>5</sup> Department of Civil and Structural Engineering, The University of Sheffield, Sheffield S1 3JD, UK

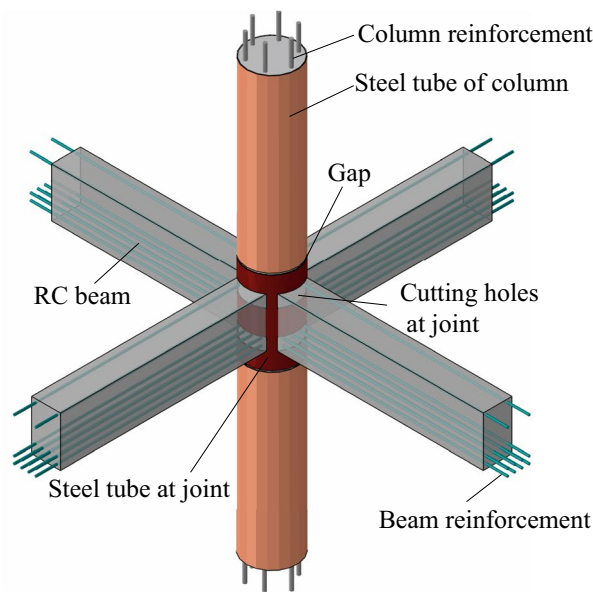


**Fig. 1** Typical configuration and engineering application of STRC columns

being utilized in engineering (Zhou & Liu, 2019). Figure 1 shows a representative application of STRC columns used in a super high-rise building in China, namely the Qingdao Haitian Tower 3 (245 m in height).

Fire performance is a crucial design consideration for STRC columns, as their steel tubes may be directly exposed to fire. To date, extensive experimental and numerical studies have been reported on the fire performance, as well as the post-fire performance, of pin-ended STRC columns with circular, square, and rectangular sections (Liu et al., 2014, 2019a, 2019b; Yang et al., 2020, 2021a; Zhang et al., 2020; Zhou et al., 2021). STRC columns have been observed to exhibit excellent performance under fire conditions. Comprehensive methods for designing the fire resistance and determining the necessary fireproof thickness of STRC columns have been developed.

In real structures, the heated STRC columns are restrained by the adjacent beams and columns. The restraints at the ends of columns in non-sway plane frames are generally categorized into axial and rotational components. The fire performance of square STRC columns with end restraints has been numerically investigated (Yang et al., 2021b). It is concluded that STRC columns with end restraints exhibit distinct behaviour compared to columns without restraints, since end restraints largely affect the internal force redistribution and buckling length of the column. Till now, no research is available concerning the fire behaviour of rectangular STRC columns with considering the end restraining effects. Compared to square STRC columns, the working mechanics of fire-exposed rectangular STRC columns is

more complex, due to the highly non-uniform distribution of confinement effect. Furthermore, the influences of axial and rotational end restraints on the fire behaviour of rectangular STRC columns may also be related to the variation of bending axis.

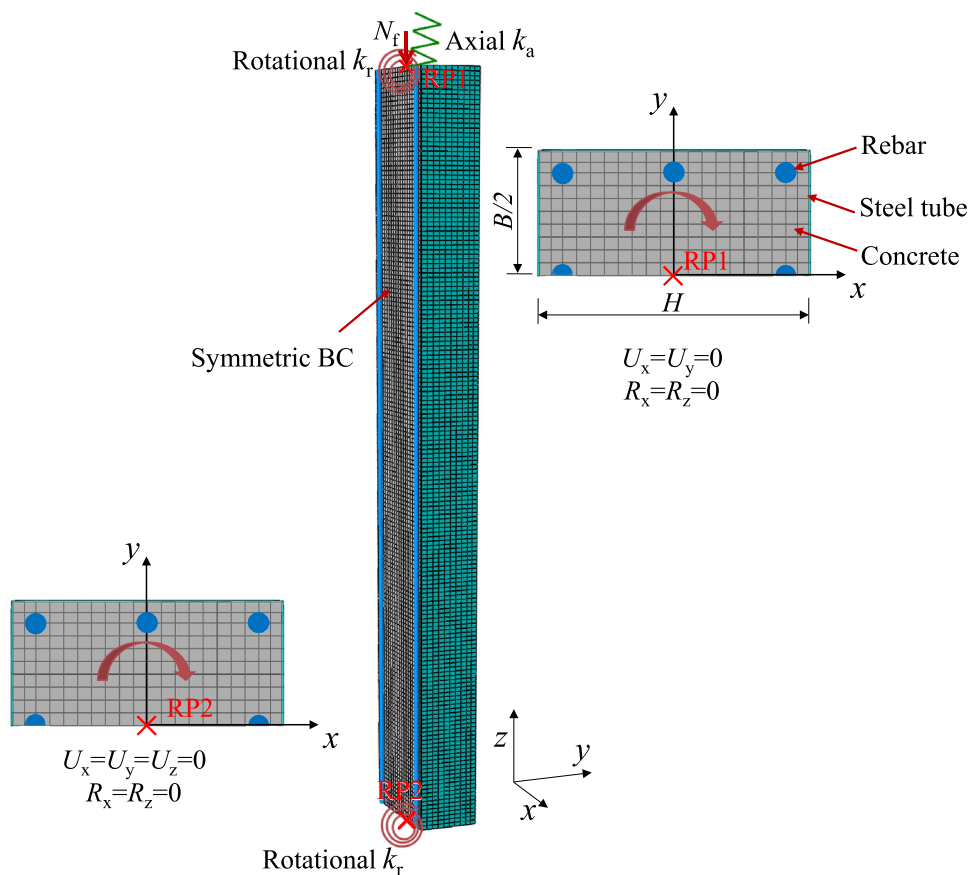
Based on the previous work (Yang et al., 2021b), this study aims to numerically investigate the fire behaviour of end-restrained rectangular STRC columns via finite element analysis (FEA). The influences of axial restraint and rotational restraint on the evolution of deformations and internal forces during heating as well as on the axial force, buckling length and fire resistance, of rectangular STRC columns with varying cross-sectional sizes, aspect ratios, slenderness ratios and load ratios were systematically analyzed through parametric studies. Finally, practical formulae were recommended for the structural fire design of rectangular STRC columns, taking into account the effects of end restraints. This study is expected to serve as a basis and contribute valuable insights for the fire performance research and design considerations of STRC columns within real framed structures, offering a reference framework for future engineering applications.

## 2 FEA Modelling

### 2.1 Model Setup

The sequentially-coupled thermo-mechanical FEA models using ABAQUS were developed to simulate the behaviour of

**Fig. 2** Finite element modelling of rectangular STRC columns with end restraints (major-axis bending)



fire-exposed rectangular STRC columns with end restraints. Considering the symmetries of loading conditions and geometric dimensions, only half of the column section was modelled, as shown in Fig. 2. The axial and rotational restraints were modelled using the Spring 1 elements in ABAQUS. Each spring was connected to the reference point at one end, and the other end was fixed. Rotational springs were assigned at the two ends of the column, while the axial spring was located only at one end of the column.

In engineering practice, a heated STRC column is typically subjected to the combined effects of axial and unequal rotational restraints at its upper and lower ends. Furthermore, the restraints at the column ends may vary with temperature due to the direct or indirect fire exposure of the surrounding members. This paper, as an initial study, primarily focuses on columns with constant end restraints. The axial and rotational restraints were investigated separately and the upper and lower rotational restraints were assumed to be equal in this research. The effects of end restraint were only taken into consideration in the mechanical analysis as it did not affect the heat transfer results.

Two normalized ratios  $\alpha$  and  $\beta$  were used to quantify the axial and rotational restraining effects at column ends, as

expressed in Eq. (1) and Eq. (2), respectively.  $\alpha$  (or  $\beta$ ) was defined as the ratio between the axial (or rotational) restraint stiffness  $k_a$  (or  $k_r$ ), provided by adjacent columns and beams at room temperature, to the ambient-temperature compression (or flexural) stiffness  $k_{ac}$  (or  $k_{rc}$ ) of the heated STRC column. In accordance with the previous recommendation (Yang et al., 2021b), the investigated scope of  $\alpha$  was 0 to 0.1, and  $\beta$  was set between 0 to 0.5.

$$\alpha = k_a/k_{ac} \tag{1}$$

$$\beta = k_r/k_{rc} \tag{2}$$

where  $k_{ac}$  ( $= (E_c A_c + E_b A_b)/L$ ) is the ambient-temperature axial stiffness of the STRC column;  $k_{rc}$  ( $= 4(E_c I_c + E_b I_b + E_s I_s)/L$ ) is the ambient-temperature rotational stiffness of the STRC column;  $E_c$ ,  $E_b$  and  $E_s$  are the elastic moduli of the concrete, rebar and steel tube, respectively;  $A_c$  and  $A_b$  are the cross-sectional areas of the concrete and rebars, respectively;  $I_c$ ,  $I_b$  and  $I_s$  are the second moments of area of the concrete, rebars and steel tube with respect to the centroidal axis of the composite section, respectively;  $L$  is the column height.

To enable comparison, rectangular STRC columns with different aspect ratios  $k_i$  (the ratio between the height  $H_i$  and width  $B_i$  of the section), but with the same cross-sectional area and steel ratio, together with an equivalent square column with width  $D_{eq}$  ( $H_i \cdot B_i = D_{eq}^2$ ) were investigated. Values of 1.2, 1.5, 1.8 and 2.0 were used for  $k_i$ , following the maximum aspect ratio regulations for rectangular CFST columns given in the Chinese design specification CECS 159 (2004). As presented in Fig. 3, the rectangular STRC columns were labelled as  $Rk_i$ -Maj and  $Rk_i$ -Min, based on their respective bending axes. While varying the aspect ratios and bending axes, the slenderness ratio of the columns remained constant. The default values of other parameters were: concrete cube compressive strength of 50 MPa, steel tube yield strength of 355 MPa, yield strength of reinforcing bar of 335 MPa, steel tube ratio of 3%, reinforcement ratio of 4%, and a concrete cover of 25 mm for the reinforcement. Given that the fire behaviour of restrained STRC columns is mainly affected by the end restraint levels (Yang et al., 2021b), fixed steel tube ratio and reinforcement ratio were adopted in this study. The values of these two parameters were selected following the regulations specified in the Chinese design standard JGJ/T471 (2020). Considering the negligible influence of stirrups on the fire resistance of STRC columns, as concluded in prior research (Yang et al., 2020, 2021a), only longitudinal reinforcements were incorporated in the FEA model. The arrangement, sizes and spacing of reinforcing bars for each cross-section, were determined according to the dimension of the composite section, the reinforcement ratio, the steel tube thickness and the concrete cover. The parameters of the FEA models constructed and analyzed in the presented numerical investigation are summarized in Table 1.

All the columns were uniformly heated along their entire heights, following the ISO 834 standard fire regime. Other details of the FEA models, e.g. the material properties, interaction and constraint, element types and meshing, were the same as those used in the previous study (Yang et al., 2021b) and were not repeated here. Currently, there are no specific definitions related to the fire resistance of end-restrained composite columns. To remain consistent with the previous work (Yang et al., 2021b), the criteria for unrestrained

column specified in (ISO834–1, 1999) are used. The fire limit state of a restrained column is reached when the axial deformation exceeds  $L/100$  or when the deformation rate reaches  $3L/1000$  mm/min ( $L$  is in mm).

## 2.2 Model Validation

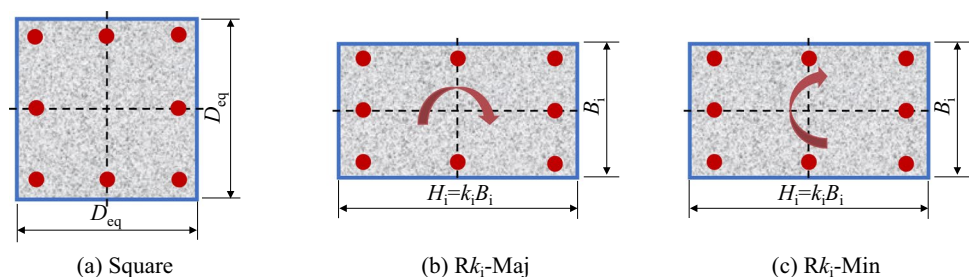
The authors have performed extensive FEA on the fire performance of 11 STRC columns and 23 CFST columns with pin-ended conditions (Yang et al., 2020, 2021a), utilizing the models developed in Sect. 2.1. Owing to the fact that there are currently no fire tests available for end-restrained STRC columns, the FEA models were validated against the test data of 34 CFST columns with axial and rotational restraints (Pires et al., 2012; Rodrigues & Laim., 2017a; Rodrigues & Laim., 2017b). Detailed comparison results between the modelled and measured data of the developments of temperature, axial deformation and restraining force, have been reported by the authors (Yang et al., 2021b).

Figure 4 shows the summarization of the ratios between the FEA-modelled critical time  $t_{cr,F}$ , the axial force ratio

**Table 1** Parameters of the FEA models constructed and analyzed in this study

Parameters	Values
Axial restraint ratio $\alpha$	0, 0.01, 0.03, 0.05, 0.1
Rotational restraint ratio $\beta$	0, 0.005, 0.01, 0.02, 0.03, 0.05, 0.1, 0.3, 0.5
Aspect ratio $k$	1.0, 1.2, 1.5, 1.8, 2.0
Equivalent width $D_{eq}$ (mm)	400, 600, 1000, 1500
Load ratio $n$	0.3, 0.5, 0.6, 0.7
Slenderness ratio $\lambda$	30, 50
Cube compressive strength of concrete $f_{cu}$ (MPa)	50
Yield strength of steel tube $f_y$ (MPa)	355
Yield strength of reinforcing bar $f_b$ (MPa)	335
Steel tube ratio $\alpha_s$	3%
Reinforcement ratio $\rho$	4%

**Fig. 3** Illustration and naming of rectangular STRC sections



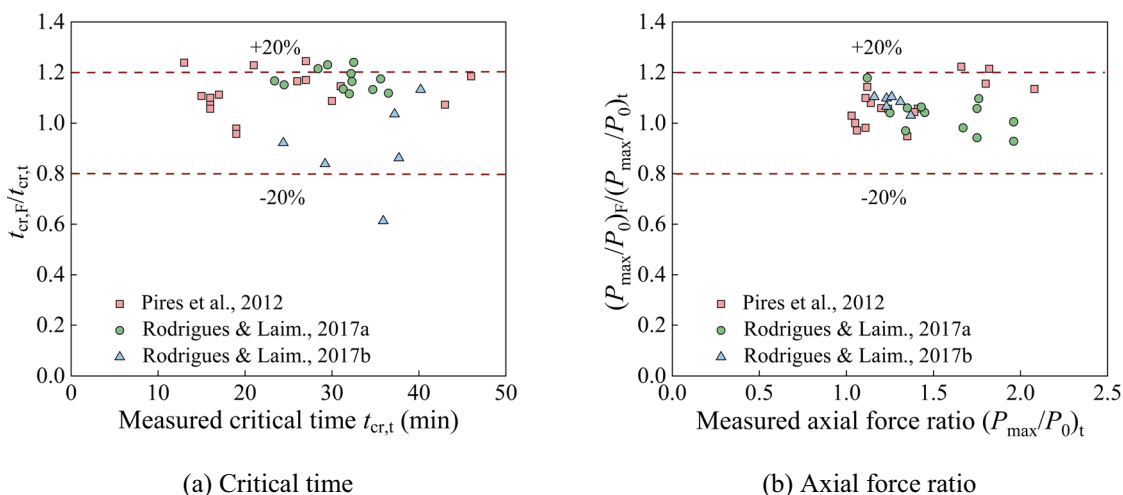


Fig. 4 Validation of the FEA model using the test data of end-restrained CFST columns

$(P_{max}/P_0)_F$  ( $P_{max}$  is the maximum force in the column during heating and  $P_0$  is the initial axial load) and the corresponding experimental data  $t_{cr,t}$  and  $(P_{max}/P_0)_t$ . The ratios  $t_{cr,F}/t_{cr,t}$  and  $(P_{max}/P_0)_F/(P_{max}/P_0)_t$  generally fall within the range of  $\pm 20\%$  and achieve mean values of 1.09 and 1.06, respectively. The discrepancies between the FEA and measured data may be attributed to the complexity of fire tests, as well as variations in end restraint stiffness and material properties utilized in the FEA simulations compared to the actual tests. Given the high variability of fire resistance tests, the FEA model is deemed adequate in simulating the performance of end-restrained composite columns. Therefore, it is confidently employed in the subsequent analysis.

### 3 Effects of Axial Restraints

#### 3.1 Discussions of Results

The influences of axial restraints on the fire behaviour of rectangular STRC columns are first assessed. It should be noted that when the restraint ratio remains constant, the applied axial stiffness differs for rectangular STRC columns with various aspect ratios and bending axes. This arises from the fact that columns with identical cross-sectional areas but different aspect ratios possess distinct axial stiffness characteristics.

Figure 5 gives typical axial deformation versus heating time curves for rectangular STRC columns with an equivalent cross-section width  $D_{eq}$  of 600 mm, a slenderness ratio  $\lambda$  of 30 and a load ratio  $n$  of 0.5. The axial load ratio of a

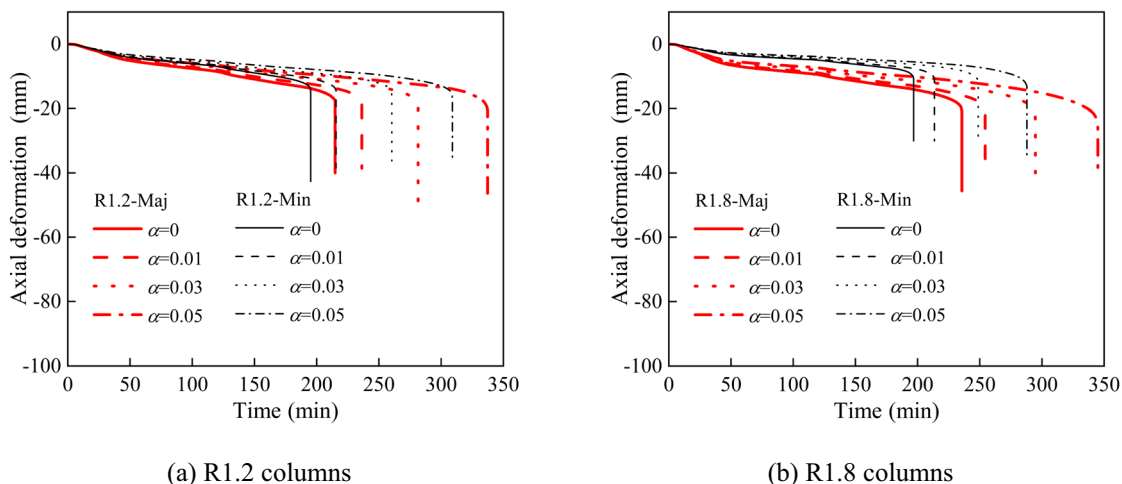
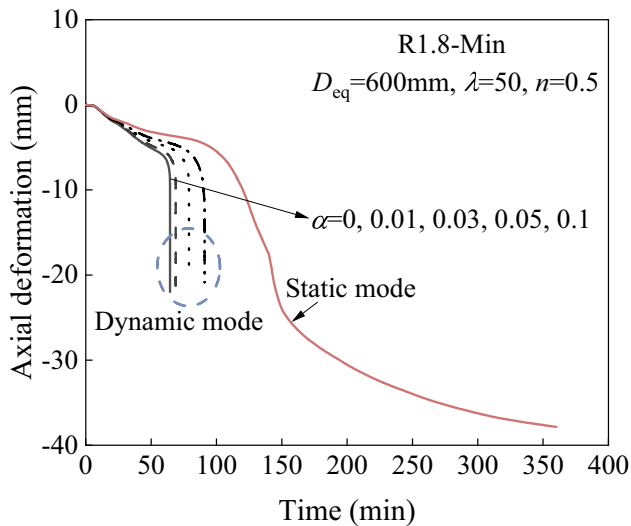


Fig. 5 Axial deformation-time curves of rectangular STRC columns with various axial restraint ratios ( $D_{eq} = 600$  mm,  $n = 0.5$ ,  $\lambda = 30$ )





**Fig. 6** Transition of failure modes for rectangular STRC columns with various axial restraint ratios ( $D_{eq}=600$  mm,  $n=0.5$ ,  $\lambda=50$ )

STRC columns is defined as the ratio between the constant load initially applied onto the column before heating and the column's ambient-temperature buckling capacity that determined following the method given in JGJ/T471 (2020). Regardless of the bending axis, both the axial deformation and its rate decrease as the axial restraint ratio increases for columns with aspect ratios of 1.2–1.8. This aligns with the findings observed in end-restrained square STRC columns (Yang et al., 2021b). As expected, the rectangular STRC column subjected to bending around the major axis exhibits a greater axial deformation compared to the case of minor-axis bending.

Most of the axially-restrained columns investigated in this study experience the failure caused by the runaway of axial

deformation, a dynamic mode. However, for slender rectangular STRC columns with relatively large axial restraint stiffness (e.g.  $\alpha=0.1$  in Fig. 6 for the R1.8-Min column with  $D_{eq}=600$  mm,  $\lambda=50$ ,  $n=0.5$ ), the failure mode may be transferred from dynamic to static, indicating the progressive collapse of the whole structures in fire could be effectively minimized (Jiang & Li., 2017).

As shown in Fig. 5, the rectangular STRC columns examined in this research experience predominantly axial contraction during heating. A portion of the applied axial load is transferred to the spring, resulting in a reduction of the axial force within the column. In this study, the concept of axial force ratio is introduced, which refers to the ratio between the time-varying axial force within the column and its buckling resistance at ambient temperature. Figure 7 presents the relationships between the FEA-outputted axial force ratio and heating time for the representative columns illustrated in Fig. 5. As the level of axial restraint increases, the axial force ratio decreases, and the descending rate of axial force increases simultaneously. This indicates a substantial improvement in the positive influence of axial restraint on the fire performance of the column. It is also noted that the vibration of the bending axis has a minimal effect on the axial force ratio of the column. This is primarily because the load ratio and axial restraint ratio remain constant for columns with varying bending axes.

The influences of axial restraint ratios on the fire resistance of rectangular STRC columns with different aspect ratios (1.2–1.8), bending axes (major- and minor-), equivalent widths (400–1500 mm), slenderness ratios (30–50) and load ratios (0.3–0.7) are presented in Fig. 8. The increase in axial restraint ratio leads to an almost linear increase in fire resistance. In general, when subjected to major-axis bending, the rectangular STRC column tends to exhibit higher fire resistance compared to a minor-axis bending counterpart.

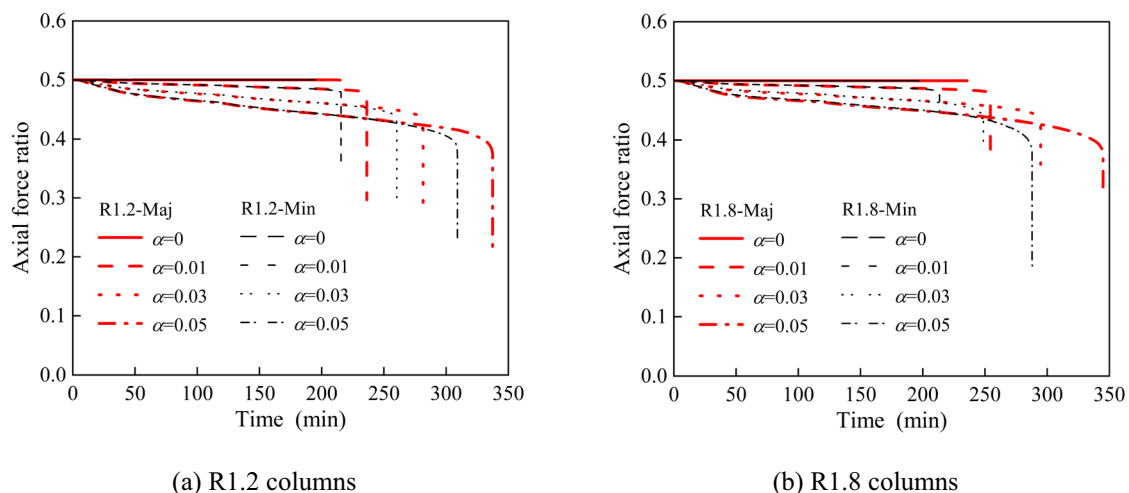


**Fig. 7** Axial force ratio-time curves of rectangular STRC columns with various axial restraint ratios. ( $D_{eq}=600$  mm,  $n=0.5$ ,  $\lambda=30$ )

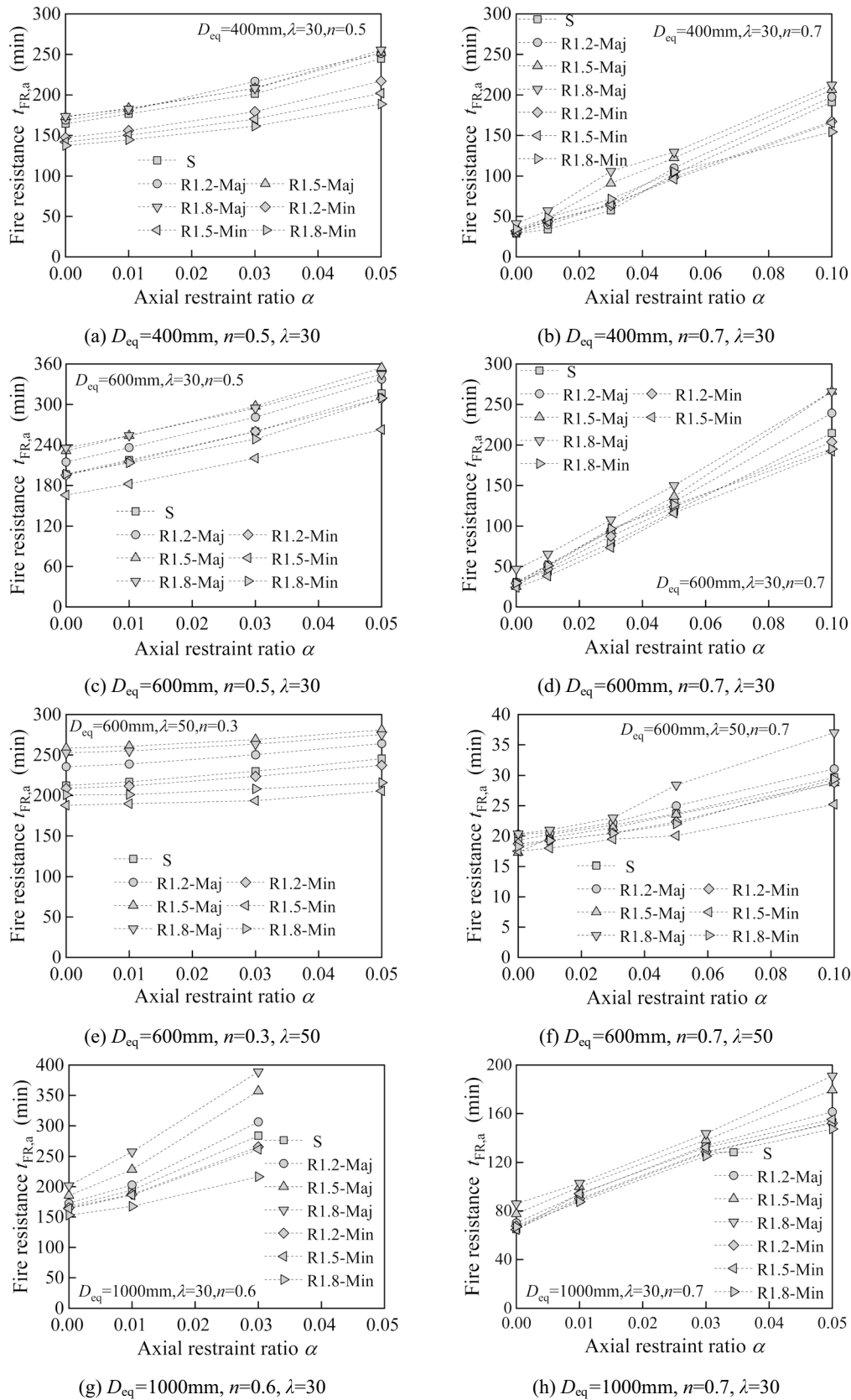


Fig. 8 Fire resistance of rectangular STRC columns subjected to various axial restraints

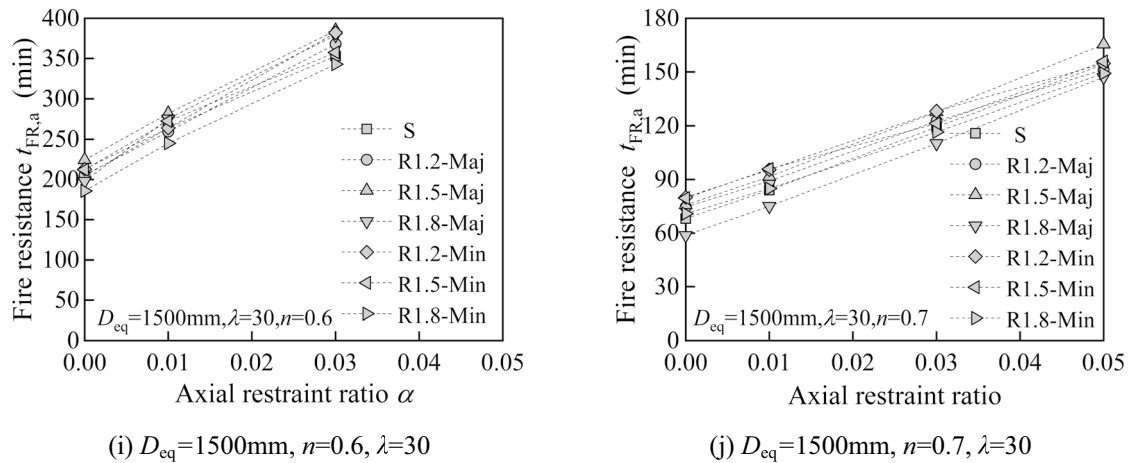


Fig. 8 (continued)

The axial force ratio of the column at the fire limit state is named as limit axial force ratio  $n_f$ . The calculation results of  $n_f$  for columns with various parameters are extracted from FEA and depicted in Fig. 9. Similar to the observation in end-restrained square STRC columns (Yang et al., 2021b), the limit axial force ratios of axially-restrained rectangular STRC columns also exhibit a near-linear decrease as axial restraint stiffness increases. Both the sectional aspect ratio and bending axis hardly affect the limit axial force ratio of the columns.

### 3.2 Design Methods

Different from pin-ended columns, rectangular STRC columns with axial restraints fail in fire when the high-temperature buckling resistance  $N_{b,T}$  decreases to the axial force inside the column during heating, as illustrated in Fig. 10. This explains why the fire resistance  $t_{FR,a}$  of axially-restrained STRC columns is extended compared to that  $t_{FR,p}$  of the unrestrained column. It is crucial to consider the influences of axial restraints when designing the fire safety of rectangular STRC columns in frame structures. The corresponding failure criterion of axially-restrained rectangular STRC columns is expressed as Eq. (3), in which  $N_{b,T}$  represents the buckling resistance at elevated temperatures that is given by Eq. (4).

$$N_{b,T}/N_b \geq n_f \quad (3)$$

$$N_{b,T} = \varphi_T N_{u,T} \quad (4)$$

where  $N_b$  and  $N_{u,T}$  are the buckling resistance at ambient temperature and compressive resistance in fire condition, respectively, which could be calculated using the previously-proposed equations (Yang et al., 2021a);  $\varphi_T$  is the high-temperature buckling reduction coefficient, which is recommended to be determined using the buckling curve (c) specified in (EN, 1993-1-1, 2005) or the square buckling curve given in JGJ/T471 (2020).

To quantitatively address the axial restraining effect on the fire performance of STRC columns, the authors have recommended a practical equation for determining the limit axial force ratio  $n_f$  of square STRC columns with axial restraints (Yang et al., 2021b), as shown in Eq. (5).

$$n_f = n - (3.6 - 0.047\lambda)\alpha \quad (5)$$

Figure 11a compares the formula-calculated limit axial force ratio using Eq. (5) and the FEA results. The average ratio between the calculated and FEA-extracted axial force ratio is 1.01, with a standard deviation of 0.03. The buckling resistance  $N_{b,T}$  of rectangular STRC columns with axial restraints is determined using Eq. (4) and compared with the limit axial force obtained from FEA modelling, and the results are shown in Fig. 11b. When using the buckling curve (c) in EC3, the average ratio between the buckling resistance and the limit axial force is 0.97, with a standard deviation of 0.08. The comparison shown in Fig. 11 demonstrates that 1) Eq. (5), which was originally proposed for square STRC columns, could be applied to rectangular STRC columns for calculating the limit axial force ratio; 2) the fire resistance of axially-restrained rectangular STRC columns could be determined by combining Eqs. (3), (4) and (5).



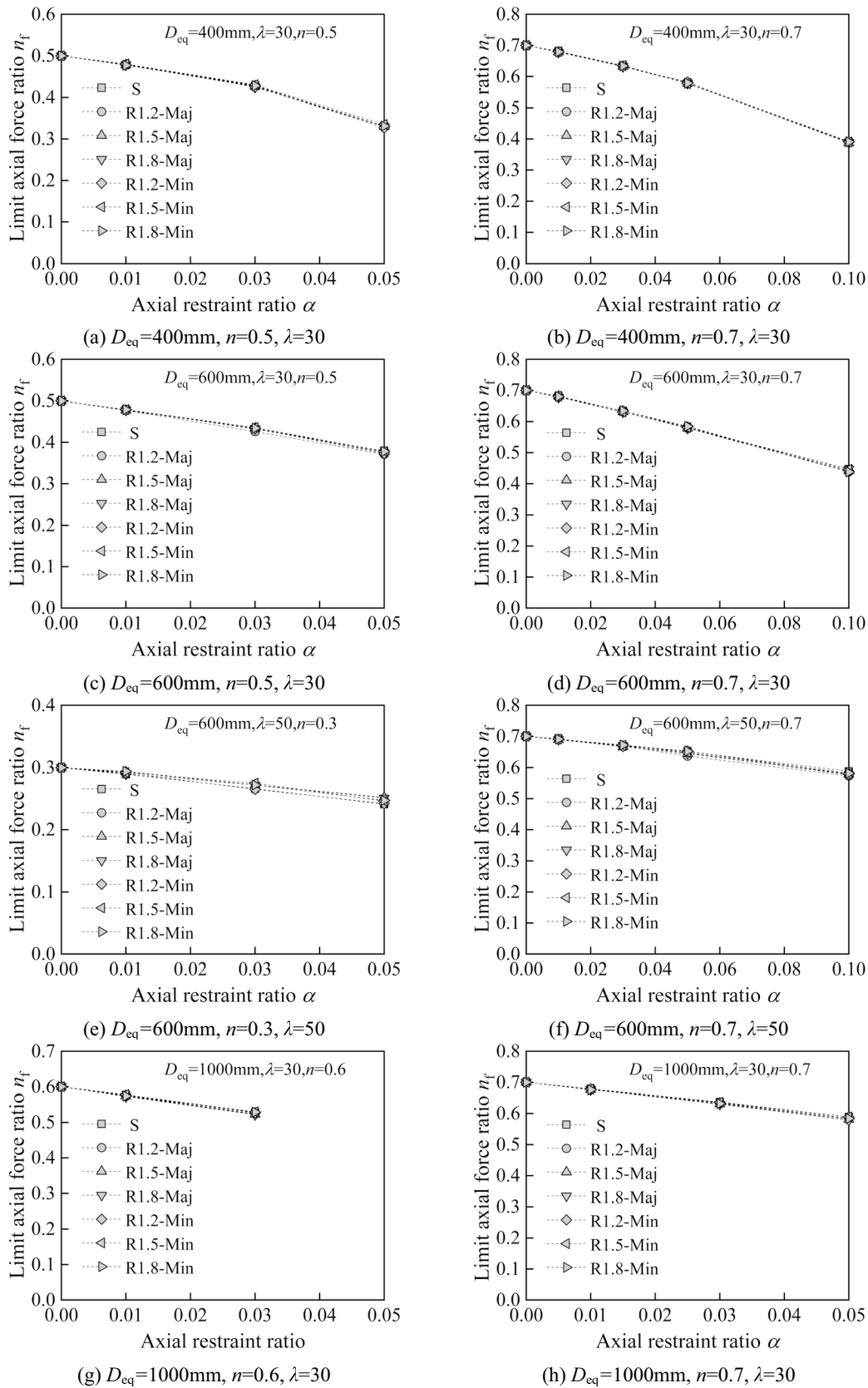


Fig. 9 Limit axial force ratios of rectangular STRC columns with different axial restraint ratios

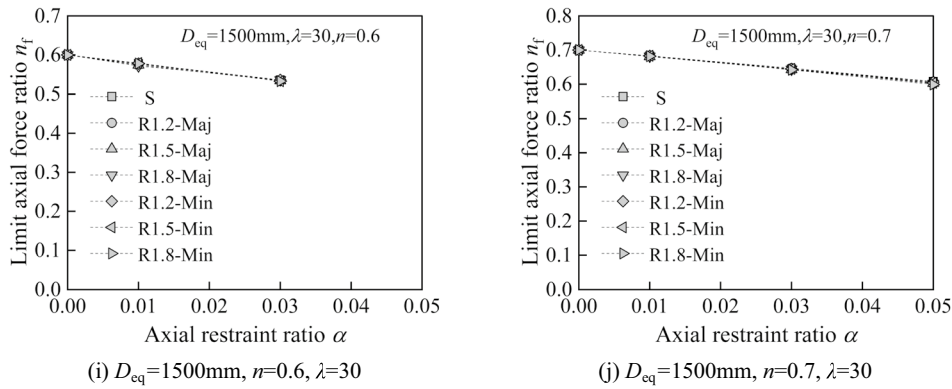


Fig. 9 (continued)

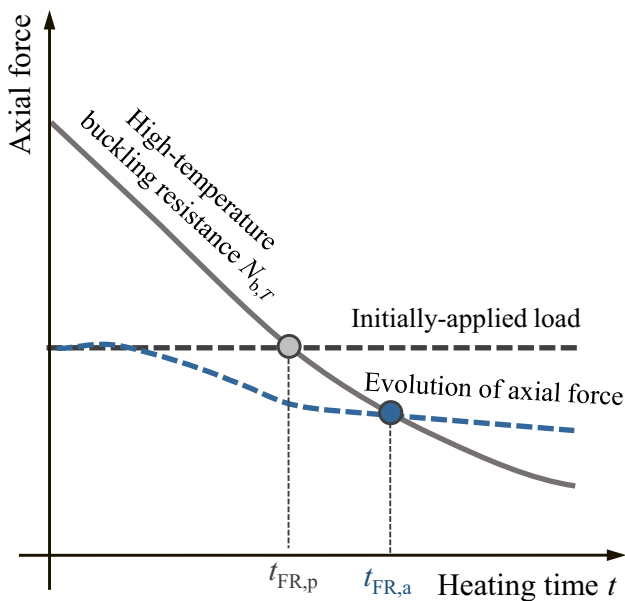


Fig. 10 Illustration for the beneficial impact of axial restraint in enhancing the fire resistance of rectangular STRC columns

## 4 Effects of Rotational Restraints

### 4.1 Discussions of Results

The main parameters investigated in this section are  $D_{eq}$  (400–1500 mm),  $\lambda$  (30–50) and  $n$  (0.5–0.7). The influences of rotational restraints on the fire resistance of rectangular STRC columns are depicted in Fig. 12. As expected, the presence of rotational restraint could effectively enhance the fire resistance of the column. In particular, the positive impact of rotational restraint is particularly noticeable when the restraint ratio is relatively low (e.g. lower than 0.1). These findings align with previous research conducted on rotationally-restrained square STRC columns (Yang et al., 2021b). Rectangular STRC columns with bending around the major axis typically exhibit larger fire resistance compared to columns with bending along the minor axis.

As the heating time increases, the buckling length of a heated STRC column gradually decreases. This is due to the reduction in the flexural stiffness of the heated column, which results in an increased level of relative restraint exerted on the column (Yang et al., 2021b). In fire-resistant

Fig. 11 Formula-calculated limit axial force ratio and buckling resistance compared to FEA results for rectangular STRC columns with axial restraints

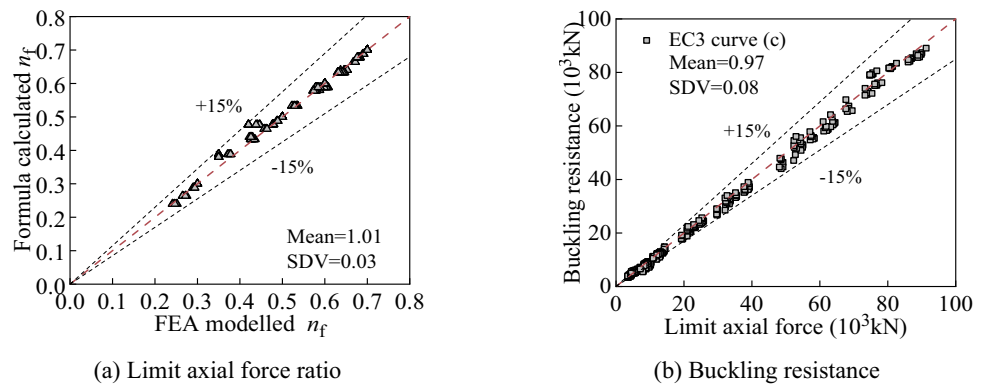


**Fig. 12** Fire resistance of rotationally-restrained rectangular STRC columns

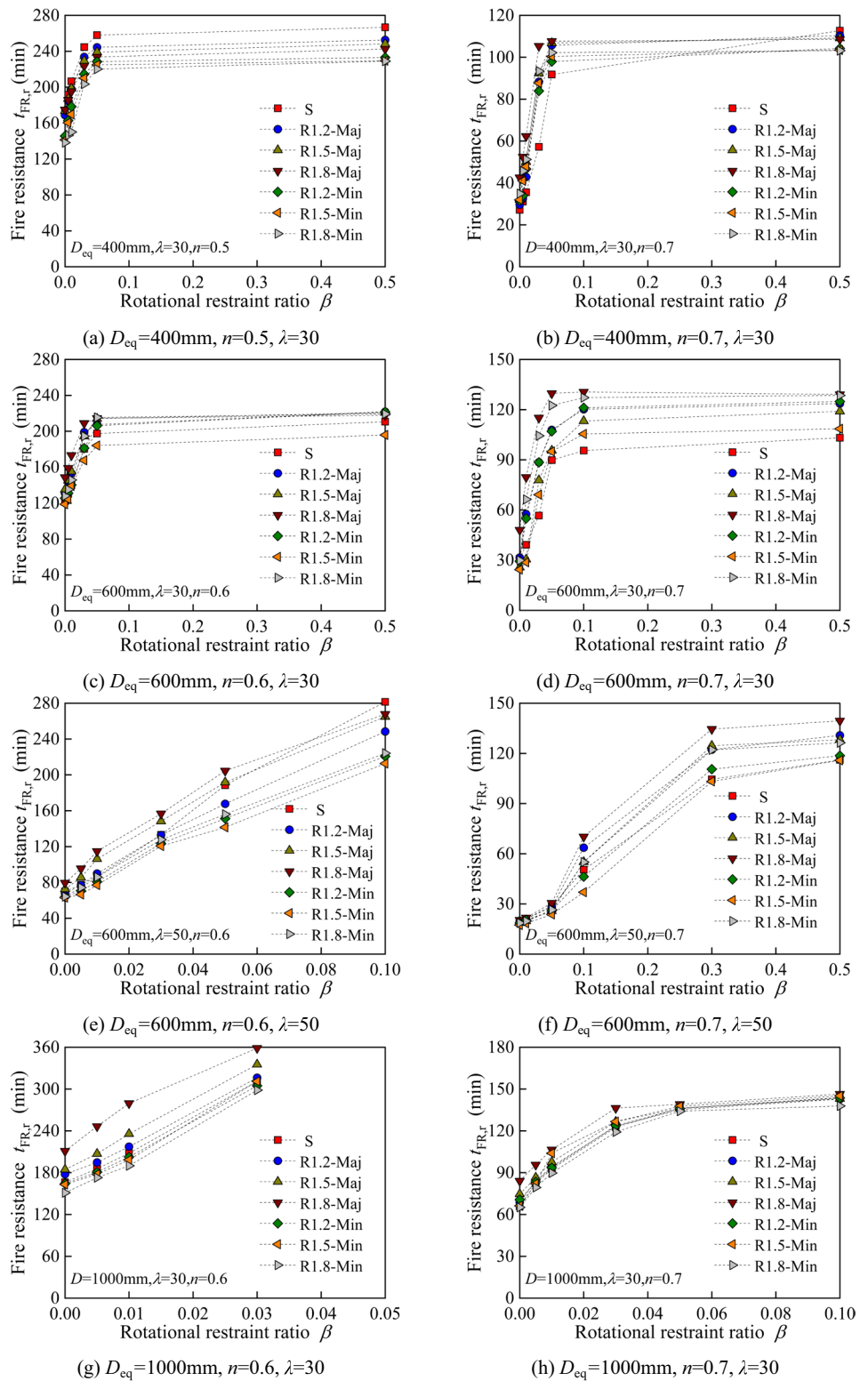
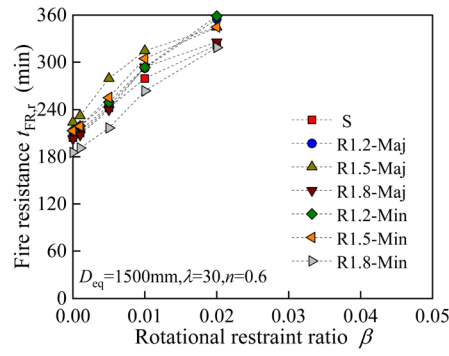
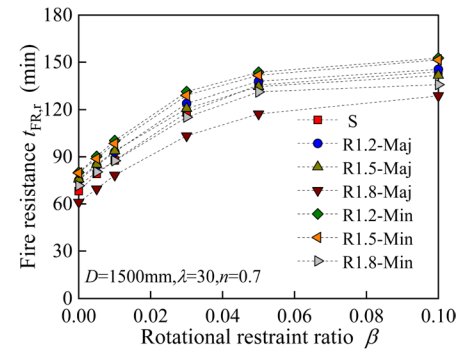


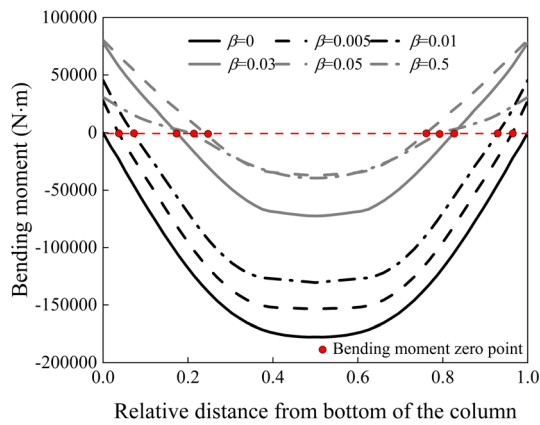
Fig. 12 (continued)



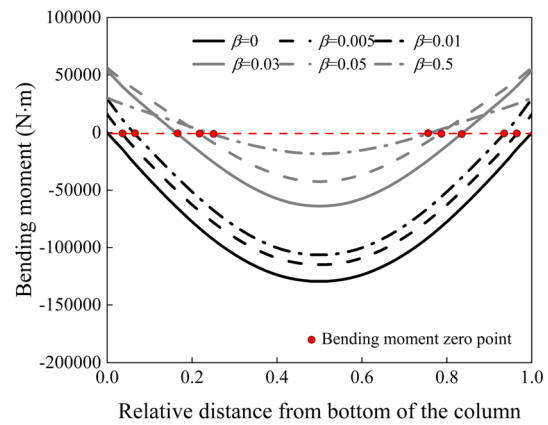
(i)  $D_{eq}=1500\text{mm}$ ,  $n=0.6$ ,  $\lambda=30$



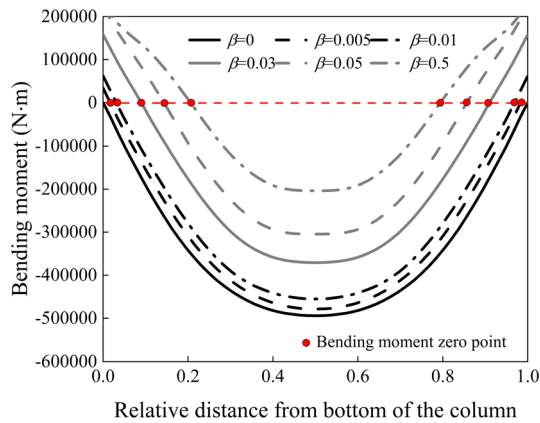
(j)  $D_{eq}=1500\text{mm}$ ,  $n=0.7$ ,  $\lambda=30$



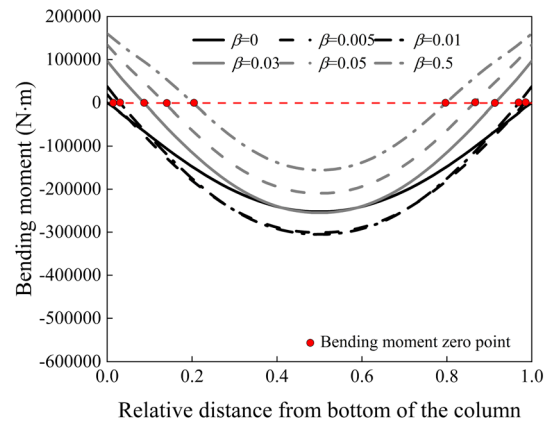
(a) R1.5-Maj ( $D_{eq}=600\text{mm}$ ,  $\lambda=30$ ,  $n=0.6$ )



(b) R1.5-Min ( $D_{eq}=600\text{mm}$ ,  $\lambda=30$ ,  $n=0.6$ )



(c) R1.5-Maj ( $D_{eq}=600\text{mm}$ ,  $\lambda=50$ ,  $n=0.5$ )



(d) R1.5-Min ( $D_{eq}=600\text{mm}$ ,  $\lambda=50$ ,  $n=0.5$ )

Fig. 13 Distributions of bending moments in rectangular STRC columns with rotational restraints at the failure state

**Fig. 14** Buckling length ratios of rotationally-restrained rectangular STRC columns

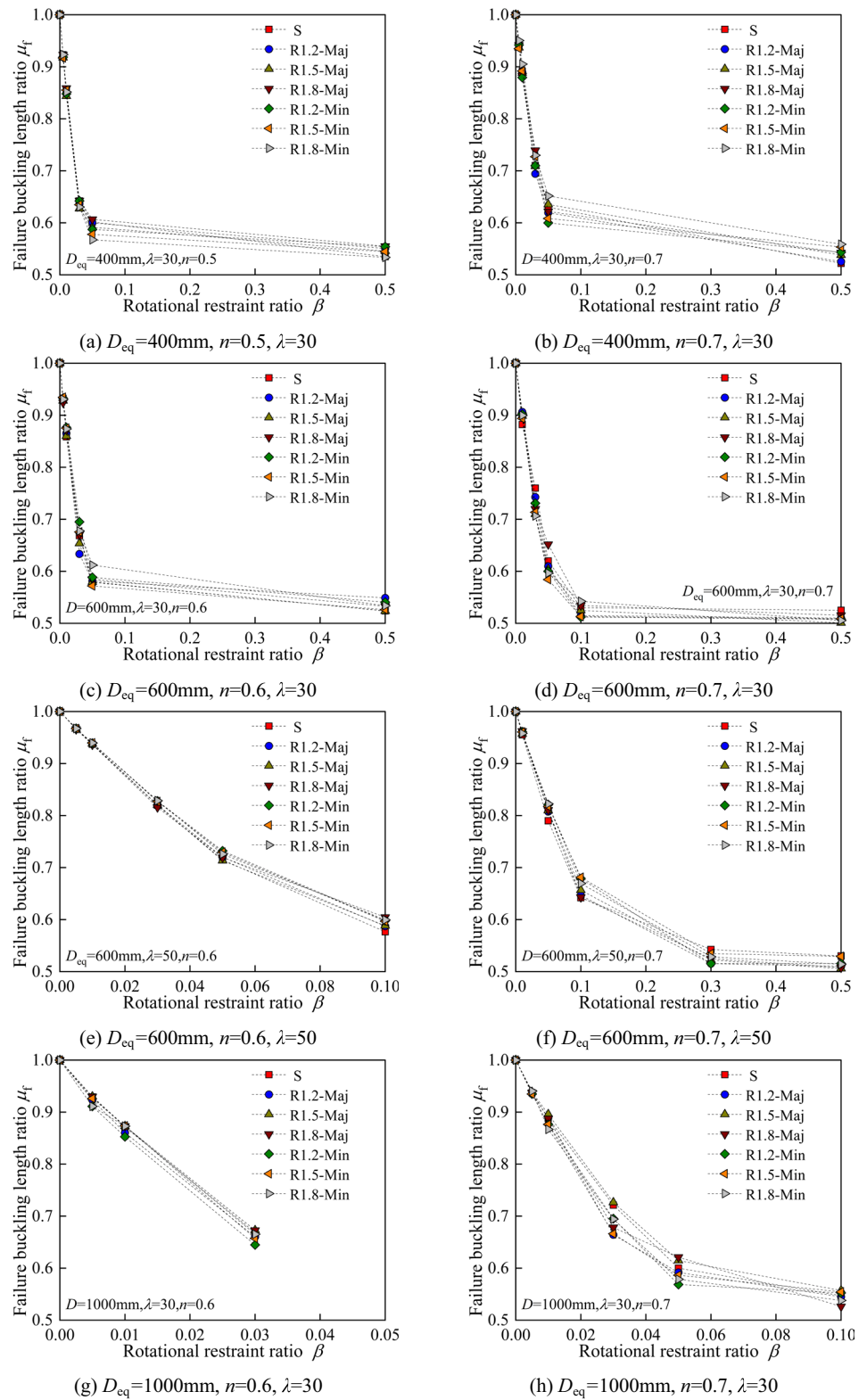




Fig. 14 (continued)

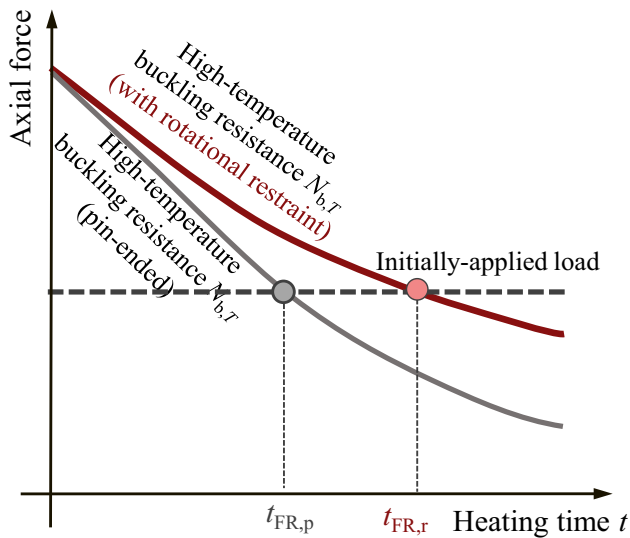
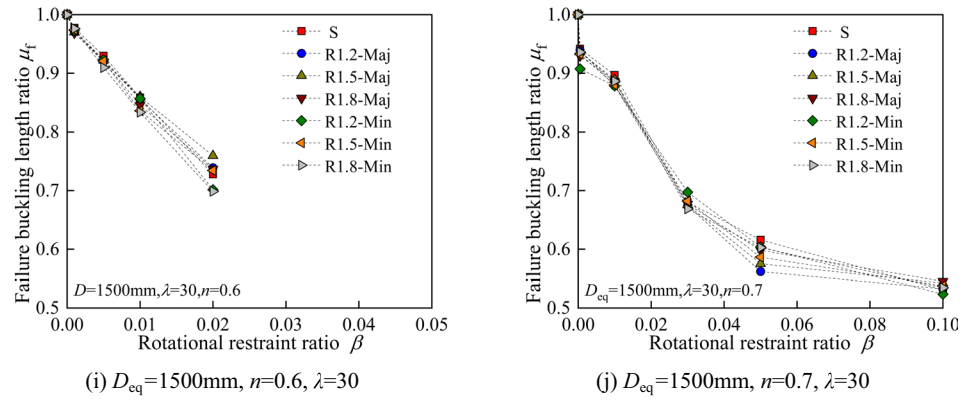


Fig. 15 Illustration for the advantageous impact of rotational restraint in improving the fire performance of rectangular STRC columns

design, it is essential to determine the high-temperature buckling length  $L_{eff}$  of the column at failure state, i.e. the distance between two bending moment zero points. These points are determined through the FEA-modelled

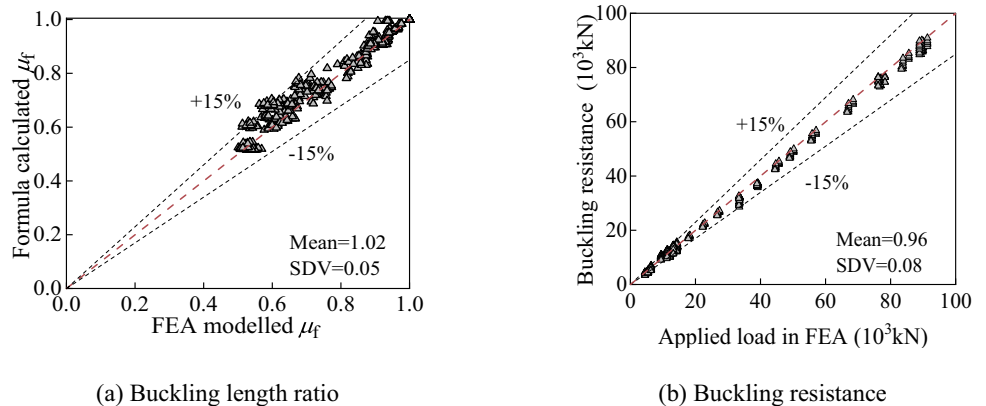
distributions of bending moment along the column height, as shown by typical examples in Fig. 13. The mid-span bending moment of the column gradually decreases as the rotational restraint increases. The rectangular STRC column with major-axis bending experiences a larger bending moment compared to the minor-axis bending case, which is primarily due to the difference in flexural stiffness between two axes.

Figure 14 presents the buckling length ratio  $\mu_f$  at failure of rectangular STRC columns with various rotational restraint ratios. The existence of rotational restraint could effectively decrease the buckling length of the column. In particular, as  $\beta$  increases from 0 to 0.5, the buckling length ratio decreases from 1.0 to around 0.5, implying the boundary condition of the column is changing from pin-ended to almost fixed. Generally, the influences of bending axis and aspect ratio on the failure buckling length ratio of the columns are marginal.

### 4.2 Design Methods

The rotationally-restrained STRC columns reach the limit state when the buckling resistance  $N_{b,T}$  decreases to the initially-applied axial load. However, the high-temperature buckling resistance of a STRC column with rotational

Fig. 16 Formula-calculated failure buckling length ratio and buckling resistance compared to FEA results for rectangular STRC columns with rotational restraints



restraint decreases at a slower rate than that of an unrestrained column. Therefore, the fire resistance  $t_{FR,r}$  of the restrained column becomes longer, as demonstrated in Fig. 15. Equation (4) is applicable to rectangular STRC columns with rotational restraints, provided that the buckling length ratio is taken into account when calculating  $\varphi_T$ .

The authors have developed a practical equation Eq. (6) to calculate  $\mu_f$  of square STRC columns with rotational restraints (Yang et al., 2021b).

$$\mu_f = \frac{1 + 0.41\beta_t}{1 + 0.82\beta_t} \quad (6)$$

where  $\beta_t = (60a_{n,D}t + 1)\beta$ ;  $a_{n,D} = 0.094/D + n - 0.46$  and  $D$  (in m) is the width of the square section.

The applicability of Eq. (6) to rectangular STRC columns with rotational restraints is evaluated by replacing the cross-sectional width  $D$  in the original formula with the equivalent width  $D_{eq}$  ( $D_{eq} = \sqrt{HB}$ ). Figure 16a compares the calculated  $\mu_f$  and the modelling results that determined using the zero-bending moment method, achieving an average ratio of 1.02 and a standard deviation of 0.05.

With Eq. (6), the buckling resistance of rectangular STRC columns with rotational restraints could be calculated using Eq. (4). The buckling reduction coefficient  $\varphi_T$  is determined in accordance with the EC3 buckling curve (c). As shown in Fig. 16b, Eqs. (4) and (6) give an accurate prediction of the buckling resistance of rotationally-restrained rectangular STRC columns in fire, achieving a mean value of 0.96 and a standard deviation of 0.08. This demonstrates that the failure buckling length ratio calculation equation Eq. (6) that previously developed for square STRC columns could be applied to the fire performance design of rectangular STRC columns with rotational restraints, just by using the equivalent cross-sectional width.

## 5 Conclusions

This study presents numerical investigations to understand the behaviour of end-restrained rectangular STRC columns in fire conditions. The effects of end restraints on the axial deformation, axial force, buckling length, as well as fire resistance of the columns, are obtained via FEA modeling. The following conclusions are drawn:

1. As the axial restraining effect increases, the failure mode of rectangular STRC columns transitions from a dynamic mode to a static mode. Both axially- and rotationally-restrained rectangular STRC columns exhibit better fire performance than unrestrained columns.
2. With an increasing axial restraint, the column demonstrates an almost linear increase in fire resistance, while

the limit axial force decreases approximately linearly. As the rotational restraint increases, the buckling length ratio of the column at the failure state decreases from 1 to 0.5, and the fire resistance is significantly prolonged, which is particularly prominent when the restraint ratio is no larger than 0.1.

3. Rectangular STRC columns that experience major-axis bending generally exhibit higher fire resistance than columns subjected to bending around the minor axis. The influences of aspect ratio and bending axis on the axial force ratio and buckling length ratio at the failure state of end-restrained rectangular STRC columns are negligible.
4. The equations given for the limit axial force ratio and failure buckling length ratio, along with the previous methods for unrestrained columns (Yang et al., 2021a), provide an approach for designing the fire performance of rectangular STRC columns with either axial or rotational restraints.

This study serves as a valuable reference for the performance-based fire safety design of STRC structures. Ongoing research is being carried out to further explore the fire behaviour of end-restrained rectangular STRC columns. This includes considering unequal rotational restraints at two ends, combining axial and rotational restraints, and incorporating time-varying restraining effects.

**Acknowledgements** The authors gratefully acknowledge the National Natural Science Foundation of China (52308534), the Natural Science Foundation of the Jiangsu Province of China (BK20220592), the Zhejiang Engineering Research Center of Intelligent Urban Infrastructure (UI2023-YB-10) and the Open Project Program of Guangdong Provincial Key Laboratory of Intelligent Disaster Prevention and Emergency Technologies for Urban Lifeline Engineering (2022ZB05), for the financial support.

**Funding** National Natural Science Foundation of China, 52308534, Dongdong Yang, Natural Science Foundation of Jiangsu Province, BK20220592, Dongdong Yang, Zhejiang Engineering Research Center of Intelligent Urban Infrastructure, UI2023-YB-10, Dongdong Yang, Open Project Program of Guangdong Provincial Key Laboratory of Intelligent Disaster Prevention and Emergency Technologies for Urban Lifeline Engineering, 2022ZB05, Dongdong Yang

## Declarations

**Conflict of interest** The authors declare there are no financial or non-financial interests that are directly or indirectly related to the work submitted for publication.

## References

- CECS 159 (2004). Technical Specification for Structures with Concrete-filled Rectangular Steel Tube Members, CECS (China

- Association for Engineering Construction Standardization), Beijing, China. (In Chinese)
- EN 1993-1-1 (2005). Eurocode 3 - Design of Steel Structures - Part 1-1: General Rules and Rules for Buildings, CEN, Brussels
- ISO 834-1 (1999). Fire Resistance Test - Elements of Building Construction, Part 1: General Requirements, International Organization for Standardization ISO 834, Geneva, Switzerland
- JGJ/T471 (2020). Technical Standard for Steel Tube Confined Concrete Structures, MOHURD (Ministry of Housing and Urban-Rural Development of the People's Republic of China), Beijing, China. (In Chinese)
- Jiang, J., & Li, G. Q. (2017). Progressive collapse analysis of 3D steel frames with concrete slabs exposed to localized fire. *Engineering Structures*, *149*, 21–34.
- Liu, F. Q., Gardner, L., & Yang, H. (2014). Post-fire behaviour of reinforced concrete stub columns confined by circular steel tube. *Journal of Constructional Steel Research*, *102*, 82–103.
- Liu, F. Q., Wang, Y. Y., Gardner, L., & Varma, A. (2019a). Experimental and numerical studies of reinforced concrete columns confined by circular steel tubes exposed to fire. *Journal of Structural Engineering*, *145*(11), 04019130.
- Liu, F. Q., Yang, H., Yan, R., & Wang, W. (2019b). Experimental and numerical study on behaviour of square steel tube confined reinforced concrete stub columns after fire exposure. *Thin-Walled Structures*, *139*, 105–125.
- Pires, T. A. C., Rodrigues, J. P. C., & Silva, J. J. R. (2012). Fire resistance of concrete filled circular hollow columns with restrained thermal elongation. *Journal of Constructional Steel Research*, *77*(10), 82–94.
- Rodrigues, J. P. C., & Laím, L. (2017a). Fire resistance of restrained composite columns made of concrete filled hollow sections. *Journal of Constructional Steel Research*, *133*, 65–76.
- Rodrigues, J. P. C., & Laím, L. (2017b). Fire response of restrained composite columns made with concrete filled hollow sections under different end-support conditions. *Engineering Structures*, *141*, 83–96.
- Yang, D. D., Liu, F. Q., Huang, S., & Yang, H. (2020). ISO 834 standard fire test and mechanism analysis of square tubed-reinforced-concrete columns. *Journal of Constructional Steel Research*, *175*, 106316.
- Yang, D. D., Liu, F. Q., Huang, S., & Yang, H. (2021a). Structural fire safety design of square and rectangular tubed-reinforced-concrete columns. *Structures*, *29*, 1286–1321.
- Yang, D. D., Liu, F. Q., Huang, S., & Yang, H. (2021b). Structural behaviour and design of end-restrained square tubed-reinforced-concrete columns exposed to fire. *Journal of Constructional Steel Research*, *182*, 106675.
- Zhang, R. Z., Liu, J. P., Wang, W. Y., & Chen, Y. F. (2020). Fire behaviour of thin-walled steel tube confined reinforced concrete stub columns under axial compression. *Journal of Constructional Steel Research*, *172*, 106180.
- Zhou, X. H., & Liu, J. P. (2019). Application of steel-tubed concrete structures in high-rise buildings. *International Journal of High-Rise Buildings*, *8*(3), 161–167.
- Zhou, X. H., Liu, J. P., & Wang, X. D. (2023). *Steel Tube Confined Concrete Structures* (pp. 2–4). Beijing: Science Press.
- Zhou, X. H., Yang, J. J., Liu, J. P., Wang, S., & Wang, W. Y. (2021). Fire resistance of thin-walled steel tube confined reinforced concrete middle-length columns: Test, simulation and design method. *Structures*, *34*, 339–355.

**Publisher's Note** Springer Nature remains neutral with regard to jurisdictional claims in published maps and institutional affiliations.

Springer Nature or its licensor (e.g. a society or other partner) holds exclusive rights to this article under a publishing agreement with the author(s) or other rightsholder(s); author self-archiving of the accepted manuscript version of this article is solely governed by the terms of such publishing agreement and applicable law.